

UNDERSEA BURIED OBJECT DETECTION USING STONELEY-SCHOLTE WAVES: APPLICATION IN COHERENT NOISE

Cyril Kottenkoff, Jean-Louis Lacoume, and Jérôme Mars

Laboratoire des Images et des Signaux
961 rue de la Houille Blanche, 38402 Saint Martin d'Hères, France
email: name.surname@lis.inpg.fr, web: www.lis.inpg.fr

ABSTRACT

A new system for buried object detection at the sea floor is presented. It is an alternative to SONAR systems using Stoneley-Scholte surface waves. The general processing method was presented in a previous publication. It is a multicomponent beamforming using an array of four component sensors set on the floor to detect echoes reflected by objects. In this paper we extend the optimal reception to waves in a correlated noise field. We derive from literature results an empirical model including spatial and intercomponent correlation. We present simulations based on it. Output SNR comparisons are made in optimal and non optimal cases. Finally we discuss the pertinence of the introduced model.

1. INTRODUCTION

The detection of objects at the sea floor is a matter of much scientific research. Acoustic SONAR systems are widely used for this task. They are the object of advanced studies for buried object detection because they have very short penetration depths in the sediments. We are interested in a rather different approach using seismo-acoustic surface waves, which propagate along interfaces. They have been used on the ground and more sparsely at the sea floor. In [1], a beamforming experiment on Stoneley-Scholte waves is described. An array of vertical geophones at the sea floor is used and a broadband processing is realized. In [2], a narrow band processing is performed with three-components geophones, in order to localize a buried object in a surf zone. We have presented in [3, 4] a concept for buried object detection at the sea floor, using an array of four component sensors (measuring the pressure and the three components of the velocity). We have described the broadband processing for Stoneley-Scholte echoes detection. In this paper we analyse the problem of noise correlation in this application and derive optimal receivers.

2. SYSTEM DESCRIPTION

The object of this study is a system based on seismo-acoustic surface waves, to detect object buried beneath the sediment surface, at the sea floor. We use Stoneley-Scholte (ST) waves, which naturally propagate along solid-fluid interfaces. Their major advantages over other waves are a favorable geometrical spreading and a low velocity, giving shorter wavelengths. Moreover they have a different polarization from body waves. As described in [3, 4], the system is composed of an array of four-component (4C) sensors, and an impulsive source. Both of them are laid on the sea floor, to optimally excite ST waves and record ST echoes. The processing is decomposed into a learning step and a beamform-

ing step. In the first step we estimate the propagation features of the ST wave in the medium (See [4] for details about this). The beamforming performs the detection and localization of objects, using the estimated features.

The detection range of our system is limited by the geometrical spreading and absorption, which can be high in unconsolidated sediments. The detection strategy includes various means to raise the Signal to Noise Ratio (SNR). The beamforming relies on:

- a wideband processing to take advantage of all the object echo's energy. It is only possible with an accurate knowledge of the ST wave dispersion.
- a multicomponent processing, which takes into account the polarization of ST waves on a 4C sensor. Other kinds of waves have different polarizations. Their contribution in the beamforming is weakened by the multicomponent processing. Furthermore, using 4C sensors raises the number of useful signals (i.e. the output SNR) without extending the array.

We develop a further improvement in this paper. In [4] we focused on the signal model and presented the maximum likelihood receiver and suboptimal receivers for white additive and independent noises. Here we take into account the noise correlation in the processing to optimize the performance. In Section 3 we build the noise field model. In Section 4 the new receiver structure is derived and in Section 5 simulations results are presented and discussed.

2.1 Signal model

In this paper we use the signal model developed in [4]. n_s denotes the number of 4C sensors used. The recorded signals are

$$\mathbf{r}(t) = \mathbf{s}(t, \mathbf{x}_o) + \mathbf{b}(t), \quad (1)$$

where \mathbf{s} is the model of the expected echo and \mathbf{b} is the noise. The parameter \mathbf{x}_o represents the horizontal coordinates of the object (see Fig.1). Each term of (1) is a vector of $4n_s$ elements indexed by i (sensor index) and k (component index). One single element of \mathbf{s} is noted $s_{ik}(t, \mathbf{x}_o)$ in time and $s_{ik}(\mathbf{v}, \mathbf{x}_o)$ in frequency. \mathbf{s} is defined by

$$s_{ik}(\mathbf{v}, \mathbf{x}_o) = p_{ST_{ik}}(\mathbf{v}) s_e(\mathbf{v}) \exp\left(\frac{-2\pi j \mathbf{v} d_i(\mathbf{x}_o)}{c_{ST}(\mathbf{v})}\right). \quad (2)$$

p_{ST_i} is the 4C ST polarization vector on the i^{th} sensor, s_e is the source waveform modified by the reflection coefficient on the object. The exponential factor is the propagation delay over a total propagation distance d_i from source (\mathbf{x}_s) to sensor (\mathbf{x}_i) with a frequency-dependent velocity $c_{ST}(\mathbf{v})$ (see Fig.1). The noise $\mathbf{b}(t)$ is presented in the next sections. The

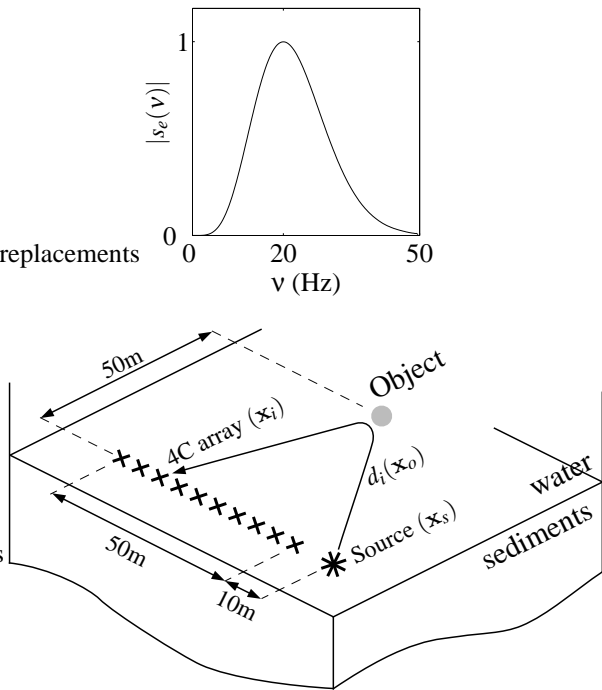


Figure 1: Normalized spectrum of the reflected wave and scenario geometry in the sea floor horizontal plane.

wave spectrum used in our simulations is presented on Fig.1 with a schematic view of the system geometry. The spectrum's maximum is at 20Hz. An empirical dispersion law was set with $c_{ST}(20\text{Hz}) = 80\text{ms}^{-1}$. We used a 50m-long linear array of 10 sensors (5.5m between sensors). The source is aligned with it 10m away and an object is simulated at a broad side position, at a 50m distance.

3. NOISE MODEL

The noise is classically considered as additive, Gaussian and centered. In this section we define the noise correlations (temporal, spatial and intercomponent) for our beamforming application. Consider for the moment a scalar noise field at the interface $b(t, \mathbf{x})$, where \mathbf{x} denotes the horizontal position. We assume ambient noise excluding for example directive ship-generated noise. It is then stationary and isotropic, we can define a spatio-temporal correlation $\Gamma_b(\tau, \mathbf{y})$, which is a function of the time delay τ and spatial distance $|\mathbf{y}|$. Some authors have studied spatial correlation of noise due to propagation in the bottom layers [1, 5]. On our experimental scale, this correlation is quite high. It should be taken into account in the processing. The publications about noise spectra on the sea floor in our frequency band are rather rare because geoscientists usually study longer periods. [6] presented however spectra up to 100Hz for geophone signals in shallow water. these spectra were rather constant from 10Hz to 100Hz. Hence it would be logical to ignore temporal correlation. In the following sections, the correlation model used is separable in space and time functions

$$\Gamma_b(\tau, \mathbf{y}) = N_b C_s(\mathbf{y}) \delta(\tau) \quad (3)$$

where N_b is the temporal Power Spectral Density (PSD), $C_s(\mathbf{y})$ is the normalized spatial correlation function derived

from [1] and $\delta(\tau)$ is the Dirac function at time delay zero. Consider now a multicomponent noise field. The four components are the x , y and z (vertical) components of the particle velocity in the medium and the pressure. They are indexed by the respective k value 1 to 4. Thanks to the noise's horizontal isotropy the two horizontal components are uncorrelated with each other and with the two others (hydrophone pressure and vertical component). This assumption is coherent with the measures in [7]. Thus we introduce four correlation functions and a cross-correlation function with an identical spatiotemporal dependence

$$\begin{aligned} \Gamma_{b_k}(\tau, \mathbf{y}) &= N_k C_s(\mathbf{y}) \delta(\tau), \quad k = 1 \dots 4, \\ \Gamma_{b_{34}}(\tau, \mathbf{y}) &= \rho_{34} \sqrt{N_3 N_4} C_s(\mathbf{y}) \delta(\tau). \end{aligned} \quad (4)$$

N_k denotes the temporal PSD on component k . Since it is known that seismo-acoustic noise at the sea floor is dominated by surface waves (ST waves in particular), the correlation coefficient ρ_{34} is given a rather high value. Indeed for a ST wave pressure and vertical velocity are coherent at the interface.

4. PROCESSING IN CORRELATED NOISE

In this section, we describe and use a beamforming adapted to coherent noise, with the noise model (4). We discretize the problem, using n_t time samples and a total signal length T . The recorded signals (1) can be rewritten

$$r_{ikt} = s_{ikt}(\mathbf{x}_o) + b_{ikt} \quad (5)$$

where i and k still denote the sensor and component indexes while t denotes now the discrete time index. If the data, model and noise are grouped in long vectors \mathbf{r} , $\mathbf{s}(\mathbf{x}_o)$ and \mathbf{b} including the time dimension (length $4n_t n_s$), the log-likelihood ratio for the parameter vector \mathbf{x}_o is

$$l(\mathbf{r}, \mathbf{x}_o) = \mathbf{s}^T(\mathbf{x}_o) \Gamma_b^{-1} \mathbf{r}. \quad (6)$$

Γ_b denotes the covariance matrix of the noise. The receiver cannot be implemented in this form because it would involve a square matrix of the size of the data (with $4^2 n_t^2 n_s^2$ elements). Equation (6) can be reformulated in the more convenient frequency domain:

$$l(\mathbf{r}, \mathbf{x}_o) = \frac{1}{n_t} \sum_{\mathbf{v}} \mathbf{s}_{\mathbf{v}}^H(\mathbf{x}_o) \gamma_{\mathbf{b}}^{-1} \mathbf{r}_{\mathbf{v}}. \quad (7)$$

In this formula superscript \mathbf{H} denotes the complex conjugate transposition. The $4n_s$ -long vectors $\mathbf{s}_{\mathbf{v}}(\mathbf{x}_o)$ and $\mathbf{r}_{\mathbf{v}}$ are the Fourier coefficients at the discrete frequency \mathbf{v} , duals of the $4n_s$ -long vectors $\mathbf{s}_t(\mathbf{x}_o)$ and \mathbf{r}_t . $\gamma_{\mathbf{b}}$ is the spectral matrix of the noise. As the beamforming is performed on many coordinates of a sea floor region, the product $\gamma_{\mathbf{b}}^{-1} \mathbf{r}_{\mathbf{v}}$ is calculated once and for all. Let it be noted $\tilde{\mathbf{r}}_{\mathbf{v}}$. With the correlation model (4) given in the previous section the elements of the discrete correlation matrix are

$$\Gamma_{\mathbf{b}_{i_1 i_2 k_1 k_2}} \tau = \mathbf{C}_{\mathbf{S}_{i_1 i_2}} \Gamma_{\mathbf{K}_{k_1 k_2}} \delta(\tau) \quad (8)$$

and those of the interspectral matrix

$$\gamma_{\mathbf{b}_{i_1 i_2 k_1 k_2 \mathbf{v}}} = \mathbf{C}_{\mathbf{S}_{i_1 i_2}} \Gamma_{\mathbf{K}_{k_1 k_2}}. \quad (9)$$

$\mathbf{C}_{\mathbf{S}i_1i_2} = C_s(\mathbf{x}_{i_1} - \mathbf{x}_{i_2})$, is the normalized spatial correlation matrix between sensors and $\mathbf{\Gamma}_{\mathbf{K}}$ is the 4×4 intercomponent covariance matrix defining the polarization of the noise.

$$\mathbf{\Gamma}_{\mathbf{K}} = \begin{pmatrix} \sigma_1^2 & 0 & 0 & 0 \\ 0 & \sigma_2^2 & 0 & 0 \\ 0 & 0 & \sigma_3^2 & \rho_{34}\sigma_3\sigma_4 \\ 0 & 0 & \rho_{34}\sigma_3\sigma_4 & \sigma_4^2 \end{pmatrix}.$$

As the processing bandwidth is n_t/T , the variance on component k is $\sigma_k^2 = N_k n_t/T$. Finally the filtered measure \tilde{r}_v is given by

$$\tilde{r}_{ikv} = \sum_{i_2} \mathbf{C}_{\mathbf{S}i_1i_2}^{-1} \sum_{k_2} \mathbf{\Gamma}_{\mathbf{K}k_1k_2}^{-1} r_{i_2k_2v} \quad (10)$$

and once written with the explicit signal model (2) the log-likelihood ratio is

$$l(\mathbf{r}, \mathbf{x}_o) = \sum_v s_{\ell v}^* \sum_i \exp\left(\frac{2\pi j v d_i(\mathbf{x}_o)}{c_{STv}}\right) \times \sum_k p_{STikv}^* \tilde{r}_{ikv}. \quad (11)$$

The following simulations implement this equation. The data are first projected on the polarization vectors of the expected ST wave (sum over k), then the spatial beamforming is computed according to the expected echo's origin (sum over i) and last the temporal matched filtering (sum over v) gives the log-likelihood ratio.

5. SIMULATIONS AND DISCUSSION

In this section, all the simulations were done with SNR equal on all the components; the noise PSD N_k were set according to this choice. The mean input SNR calculated for a given (i, k) signal is

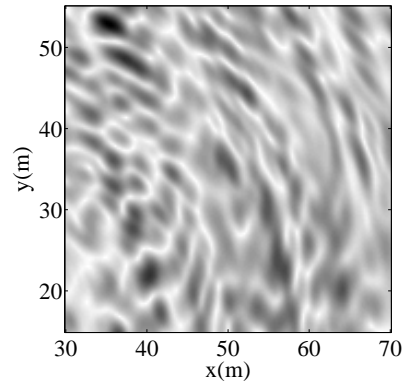
$$\text{SNR}_i = \frac{\sum_t s_{ikt}^2(\mathbf{x}_o)}{n_t \sigma_k^2}. \quad (12)$$

Without attenuation the input SNR are also independent of the object position \mathbf{x}_o . According to [8] the output SNR of the receiver is

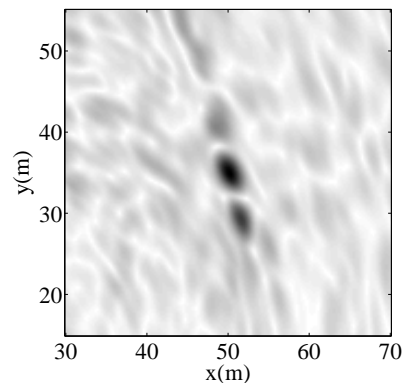
$$\text{SNR}_o = \mathbf{s}^T(\mathbf{x}_o) \mathbf{\Gamma}_{\mathbf{b}}^{-1} \mathbf{s}(\mathbf{x}_o). \quad (13)$$

On Fig.2 are displayed two beamforming images from the same data set, including a object echo and spatially correlated noise. No intercomponent correlation was modeled here ($\rho_{34} = 0$). For the first image, the noise is assumed spatially white, whereas on the second, its actual correlation is considered in the processing. We used the envelopes of the maximum likelihood receivers in order to avoid rapid oscillations on the images. Qualitatively we observe an obvious increase of the detection capacity for the adequate receiver. Quantitative comparisons are shown in table 1. For a given SNR_i , we calculated SNR_o for several noise correlations and for receivers adapted or not. The results are normalized by the optimal white noise case. In the table “ zp ” indicates an intercomponent correlation with the coefficient value $\rho_{34} = 0.9$. Important remarks can be formulated about this table:

- For each row (i.e. for each noise set) the best SNR value lies on the “diagonal” of the table. These values correspond to the three optimal cases.



(a)



(b)

Figure 2: Normalized beamforming images in a spatially correlated noise (SNR -23dB). Receiver adapted to white noise (a) and optimal receiver (b). The object's coordinates are $\mathbf{x}_o(50, 35)$ in meters.

Table 1: Normalized output SNR for several scenari.

Actual correlation	Assumed correlation		
	none	spatial	spatial and zp
none	1	0.64	0.59
spatial	1.20	8.98	8.2
spatial and zp	0.83	6.16	6.85

- The comparison of rows 2 and 3 shows that a high correlation of the pressure and vertical velocity components of the noise lowers the performance. This result is expected because a high value of ρ_{34} constrains the noise to have a closer structure to ST waves, at least in term of polarization considering these two components. For a negative value of ρ_{34} an opposite trend would be observed. As said in section 3 the seismo-acoustic noise field is dominated by surface waves. If it was exclusively composed of ST waves then the two components would be fully redundant. Thus one of them could be ignored in the detection process. Keeping both pressure and vertical velocity is useful for wave kind discrimination.
- On the contrary the comparison of rows 1 and 2 shows that giving the noise a spatial correlation $C_s(\mathbf{x})$ on simulation helps the detection, whatever the receiver structure.

In order to explain this last observation we can interpret the problem in the frequency-wavenumber ($v - k$) domain. The

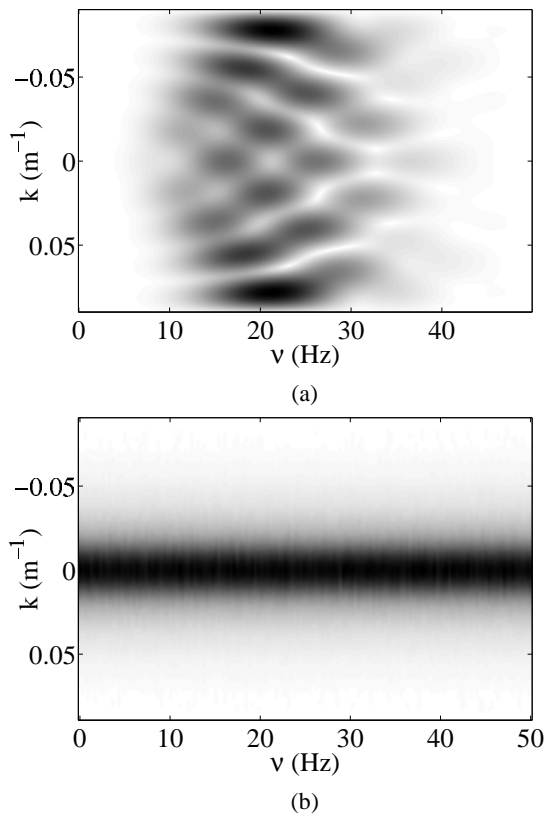


Figure 3: $v-k$ transform of the wave signal used in the simulation (a) and spatio-temporal PSD of the noise (b, one component). Both are displayed with the same $v-k$ scale.

representation of the signal and the noise in this domain provides a different distribution of the noise's power and the signal's energy. On Fig.3 are displayed the $v-k$ representation of one echo signal component and the spatio-temporal PSD $\gamma_b(v, k)$ of the noise. They are computed by 2D Fourier transforms of the signal and the spatio-temporal correlation. Since the correlation distance of the noise is quite long, the power in the spatio-temporal PSD is concentrated along the v axis. It is clearly visible that most of the wave signal's energy is on a part of the $v-k$ plane where $\gamma_b(v, k)$ is the weakest. This explains the high receiver gain with this noise model. At this point the model's pertinence may be reconsidered. The array processing performance could be overestimated because of a lack of realism. Hence it would be useful to refine it by considering physical propagation aspects such as the surface-wave nature of the noise.

6. CONCLUSION

This study deals with a new system that performs a beamforming on Stoneley-Scholte wave to detect buried objects at the seafloor. Its principle was introduced in [4]. The sys-

tem uses multicomponent sensors to take advantage of the polarization nature of the waves. We developed in this paper an extension of the maximum likelihood receiver to handle noise correlation. This correlation could be either temporal, spatial or intercomponent. We defined an empirical noise model built from literature results and we tested its influence on simulation. For given SNR, the receiver shows a little performance loss when the noise model includes an intercomponent correlation. On the contrary much greater performance is observed when spatial correlation is added. This high gain must be considered with some reserve because the model defined does not take into account the surface-wave nature of seismo-acoustic noise. Further physical modeling would be necessary to improve it. However in real experiments, the receiver developed could be applied with models estimated *in situ* for optimal detection.

REFERENCES

- [1] J. A. TenCate, T. G. Muir, A. Caiti, A. Kristensen, J. F. Manning, J. A. Shooter, R. A. Koch, and E. Michelozzi, "Beamforming on seismic interface waves with an array of geophones on the shallow sea floor," *IEEE Journal of Oceanic Engineering*, vol. 20, pp. 300–309, October 1995.
- [2] E. Smith, P. S. Wilson, F. W. Bacon, J. F. Manning, J. A. Behrens, and T. G. Muir, "Measurement and localization of interface wave reflections from a buried target," *J. Acoust. Soc. Am.*, vol. 103, pp. 2333–2343, May 1998.
- [3] C. Kotenkoff, J. L. Lacoume, and J. Mars, "Generation of seismo-acoustic surface waves for undersea buried object detection," in *Proc. of the Fourth International Conference on Physics in Signal and Image Processing*, vol. 1, (Toulouse, France), pp. 87–91, 2005.
- [4] C. Kotenkoff, J. L. Lacoume, and J. Mars, "Multicomponent seismo-acoustic surface waves beamforming for undersea buried object detection," in *Proc. of Oceans 2005 - Europe*, vol. 2, (Brest, France), pp. 769–774, 2005.
- [5] A. E. Schreiner and L. M. Dorman, "Coherence lengths of seafloor noise: Effect of ocean bottom structure," *J. Acoust. Soc. Am.*, vol. 88, pp. 1503–1514, Sept. 1990.
- [6] H. Schmidt and W. A. Kuperman, "Estimation of surface noise source level from low frequency seismoacoustic ambient noise measurements," *J. Acoust. Soc. Am.*, vol. 84, p. 21532162, Dec. 1988.
- [7] B. Schmalfeldt and D. Rauch, "Ambient and ship-induced low-frequency noise in shallow water," in *Bottom-Interacting Ocean Acoustics* (W. A. Kuperman and F. B. Jensen, eds.), vol. 5 NATO Conference Series: Marine Science, (New York), pp. 329–343, Plenum Press, 1980.
- [8] H. L. Van Trees, *Detection, Estimation, and Modulation Theory*. part 1, New York: John Wiley & Sons, 1968.